07 Jan 2009

Computed Tomographic Investigation of the Influence of Gas Sparger Design on Gas Holdup Distribution in a Bubble Column

B. C. Ong

P. Gupta

A. Youssef

M. (Muthanna) H. Al-Dahhan
Missouri University of Science and Technology, aldahhanm@mst.edu

et. al. For a complete list of authors, see https://scholarsmine.mst.edu/che_bioeng_facwork/1277

Recommended Citation

B. C. Ong et al., "Computed Tomographic Investigation of the Influence of Gas Sparger Design on Gas Holdup Distribution in a Bubble Column," *Industrial and Engineering Chemistry Research*, vol. 48, no. 1, pp. 58 - 68, American Chemical Society, Jan 2009.
The definitive version is available at https://doi.org/10.1021/ie800516s

Computed Tomographic Investigation of the Influence of Gas Sparger Design on Gas Holdup Distribution in a Bubble Column

B. C. Ong, P. Gupta, A. Youssef, M. Al-Dahhan,* and M. P. Duduković

Chemical Reaction Engineering Laboratory (CREL) Energy, Environmental and Chemical Engineering Department (EECE), Washington University, St. Louis, Missouri 63130-4899

The effect of gas sparger design on the gas holdup radial profile in a bubble column (with a diameter of 0.162 m) has been studied using γ-ray computed tomography (CT). Six different configurations of gas spargers were examined, using an air−water system for selected superficial gas velocities from 2 cm/s to 30 cm/s, covering the homogeneous and heterogeneous (churn-turbulent) flow regimes. Two operating pressures were used: 1 and 4 atm. Differences were found between the gas holdup distributions produced by different spargers at dimensionless radii of $r/R < 0.8$ in the central region of the column. The cross and single nozzle spargers produced closely similar gas holdup distributions, while the perforated plate sparger produced a higher gas holdup when compared to other spargers with the same percentage open area (POA). At 4 atm, the sparger design did not have a significant effect on the gas holdup profiles, compared to atmospheric pressure, except for the case of the single-hole sparger, which was found to yield a higher gas holdup.

1. Introduction

Bubble columns are cylindrical vessels in which gas is sparged in the form of bubbles through a distributor (sparger) into a liquid (two-phase bubble column) or a suspension of fine solid particles in a liquid (three-phase slurry bubble column). The liquid may flow co-currently or counter-currently, relative to the gas. Bubble columns can also be operated in a semibatch mode. In all cases, a high interfacial contacting area is provided. Bubble columns have been used as multiphase reactors (or contactors) in chemical, biochemical, petrochemical, wastewater treatment, and metallurgical industries. Fischer−Tropsch (FT) synthesis is especially considered to be among the important applications where bubble columns are the reactors of choice.

The flow field in bubble columns results from the complex interactions of the phases. Gas holdup and its cross-sectional distribution are among the important parameters affecting the hydrodynamics and interphase transport in these reactors. Knowledge of the gas holdup is an essential prerequisite for bubble column design.[1] In addition, gas holdup and its cross-sectional distribution or radial profile impact the liquid recirculation and backmixing.[2−4] The gas, which is introduced into bubble columns via a gas sparger at the bottom, undergoes complex dynamic changes through bubble formation, growth, detachment, and mutual bubble interactions that affect the flow field in the column.

It has been reported that the sparger design and its configuration have a significant effect on gas holdup and its radial profile only in the bubbly flow regime, and that this effect diminishes at higher superficial gas velocities (i.e., the churn-turbulent flow regime).[5−8] However, some other studies do not support this point of view. Freedman and Davidson[9] observed significant variation in the gas holdup, depending on the percentage of the distributor cross section occupied by the sparger holes. They concluded that the radial profile of the gas holdup is dependent on many factors, one of which is the design of the gas sparger.

Ueyama et al.[10] compared the effect of single and multinozzle spargers on a pilot-scale unit, using an air−tap-water system with superficial gas velocities up to 33.1 cm/s. The column had an internal diameter (D) of 60 cm and a total height (L) of 303 cm, resulting in a column aspect ratio (L/D) of 5.1. Axial profiles of the cross-sectional mean holdup were estimated using pressure taps, whereas lateral distributions of holdup and bubble velocities were obtained using an electrical resistivity probe. The aforementioned authors reported significant axial variations of gas holdup with sparger design for smaller dispersed-height-to-diameter ratios ($Ls/D < 2.2$). However, for higher Ls/D ratios (2.2−3), and at superficial gas velocities (>15.5 cm/s), insignificant axial variation in the average gas holdup was observed. When the dispersed-height-to-diameter ratio (Ls/D) was kept low at 0.58, Ueyama et al.[10] observed a significant effect of the distributors on the radial gas holdup profiles, even at a very high superficial gas velocity of 32.4 cm/s. This is to be expected, because the measurements in such a short column would invariably reflect the behavior in the distributor region.

Mikkilineni and Knickle[11] studied the effect of porous plate distributor thickness (1.59−12.7 mm) and pore size (35−70 μm) on gas holdup and flow patterns in a 15.2-cm inner diameter (ID) bubble column, using an air−water system. They conducted the study for gas superficial velocities of up to 35 cm/s and concluded that there is insignificant variation in holdup with pore size and plate thickness in the churn-slug regime. Rivas et al.[12] studied the effect on holdup using a perforated plate, mesh plate, and cone distributor in a 30-cm ID column ($L/D = 10$ and 13.3), with two organic solvents as the liquid and air as the gas phase. They measured the mean gas holdup using pressure taps for gas superficial velocities up to 18 cm/s. No significant effect of the distributor on holdup was observed, which was attributed to distributor effects being confined to the bottom region of the column near the distributor.

Tsuchiya and Nakanishi[13] studied various perforated plate configurations in a 14.8-cm-ID bubble column (column height of 802 cm) using air as the gas phase and water as the liquid phase. The study was performed for superficial gas velocities up to 54 cm/s, and the overall gas holdup was obtained based on the bed expansion method. By keeping the size of the distributor holes fixed, they found that the overall gas holdup

* To whom correspondence should be addressed. Present address: Chemical Reaction Engineering Laboratory (CREL). Energy, Environmental, and Chemical Engineering Department, Washington University, St. Louis, MO 63130. Tel.: +1(314) 935-7187. Fax: +1(314) 935-7211. E-mail address: muthanna@wustl.edu.

10.1021/ie800516s CCC: $40.75
Published on Web 12/31/2009

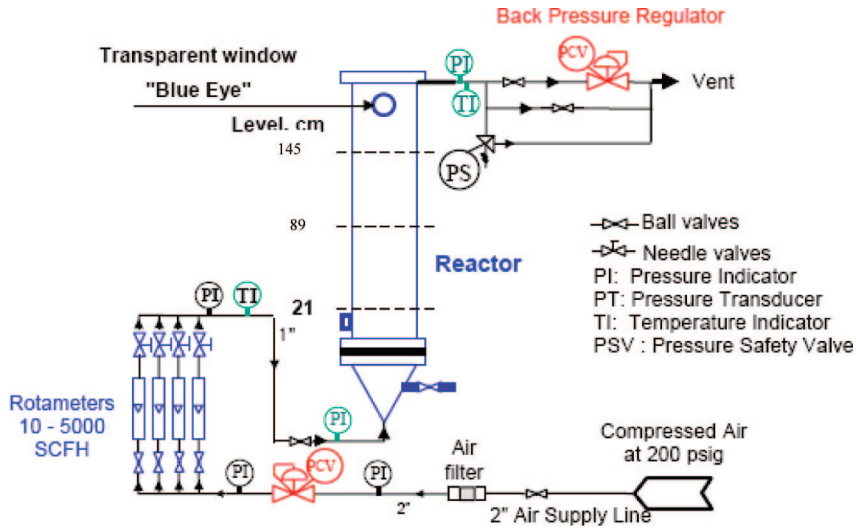

Figure 1. Schematic diagram of the experimental setup.

increased with an increased number of holes on the perforated plate. When the number of holes on the perforated plate was fixed, the average gas holdup decreased as the orifice diameter increased, provided that it was maintained between 1−2 mm. The aforementioned conclusions were based on the holdup obtained in both homogeneous and transition regimes. No significant effect of distributors was observed for gas superficial velocities of >14 cm/s, when the flow seemed to be churn-turbulent. George et al.[14] found that the effect of distributors was limited to axial levels of $z/D = 2.1$ in a 0.483-m-diameter column at $U_g = 5-30$ cm/s and $P = 0.1-0.5$ MPa. In many of these studies, the overall gas holdup was measured using either the dynamic gas disengagement (DGD) technique[7,15] or intrusive probes.[16−20] However, these measurement techniques have some shortcomings associated with measuring high gas volume fractions in transient accelerating or decelerating flows. Furthermore, little has been done to quantify the effect of sparger design on the column's hydrodynamics using reliable noninstrusive measuring techniques.

Therefore, the focus of this study is to assess the effect of sparger design on the gas holdup radial profile in a bubble column, using an advanced and noninvasive measurement technique based on γ-ray computed tomography (CT) at a range of superficial gas velocities and two pressures (1 and 4 atm).

2. Experimental Setup and Measurement Technique

The noninvasive γ-ray computed tomography (CT) technique[5] was used to measure the time-averaged cross-sectional gas holdup distribution at three axial levels ($z/D = 2.1$, 5.5, and 9) of a stainless steel bubble column. The vessel was 16.2 cm (6.4 in.) in diameter and 250 cm (8.2 ft) in height, and it was operated at selected gas superficial velocities of 2−30 cm/s and operating pressures of 1 and 4 atm. The liquid was tap water, used in a batch mode, and the dynamic liquid height was maintained at 180−200 cm above the distributor as indicated by a transparent glass window, called a "blue eye". Situated at the top of the column, the blue eye allowed viewing the system before starting the γ-ray CT scan.

Figure 1 shows the schematic of the bubble column setup used in this study, which has been designed to deliver a high flow rate of compressed air up to 5000 SCFH (142 SCMH) at a pressure of up to 150 psig. [Note: SCFH denotes standard cubic feet per hour; SCMH denotes standard cubic meters per hour.] The gas flow rate was controlled using four rotameters to cover the entire range of desirable flow rates. After exiting the bubble column, the gas passes through a backpressure regulator, which controls the pressure in the column. It is then vented into the atmosphere. Two pressure safety valves at the top and bottom of the column prevent accidental overpressurization.

Figure 2 is a schematic of the various distributors used in this study to investigate the sparger effect on gas holdup radial profiles. The design specifications and configurations of these spargers are summarized in Table 1.

The cross-sectional gas holdup distribution was measured using the γ-ray CT and the associated tomography reconstruction algorithms developed in the Chemical Reaction Engineering Laboratory (CREL), which are discussed in detail in ref 5 and reported in ref 21. The CREL scanner is a versatile instrument that enables the quantification of the time-averaged holdup distribution for two-phase flows under a wide range of operating conditions.[22−24] The fan beam configuration of the scanner consists of an array of NaI detectors 5 cm in diameter (five detectors were used in this study), and an encapsulated <100 mCi Cs^{137} source located opposite to the center of the array of detectors. The detectors and the source are mounted on a plate that can be rotated 360° around the axis of the column by a stepping motor that is controlled through a microprocessor. Moreover, the entire assembly can be moved in the axial direction along the column to scan column cross sections at different axial levels of the column. The CT scanner that was used gave a spatial resolution of ∼0.35 cm in the horizontal direction and 1.0 cm in the vertical direction. Usually, the data is collected at 20 Hz and 114 samples are recorded for each projection, yielding a total acquisition time per projection of 5.7 s. Because five detectors were used to fully cover the column diameter of 0.162 m, five projections are simultaneously acquired by these detectors at any given position of the source and detector array. At each view (i.e., a given position of the source), the detector collimator makes seven movements at 0.453° each, covering 2.72° of each detector face, acquiring five projections for each movement. A total of 35 projections ($5 \times 7 = 35$) are recorded for each. When the projection measurements of a view are completed, the plate of the source/detectors moves 3.6° to another view (i.e., another source position). Ninety-nine views (for a total of 356.4°) are acquired during each CT experiment. Hence, the CT scan for a 0.162-m diameter column lasts ∼110 min.[25]

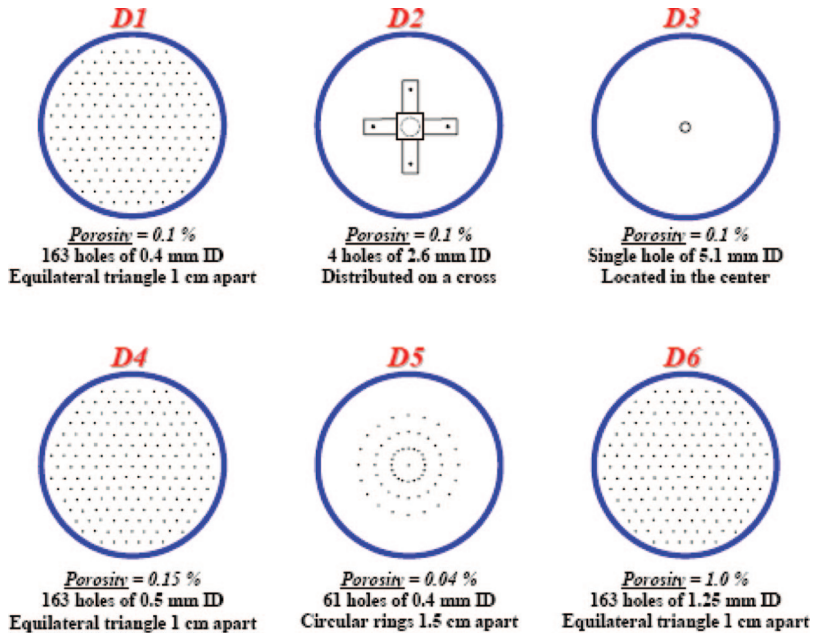

Figure 2. Sparger designs and configurations.

Table 1. Design Specification and Configuration of the Used Spargers

name	type and description
D1	perforated plate, 163 holes of 0.4 mm I, 0.1% open area, equilateral triangle 1 cm apart
D2	cross sparger, 4 holes of 2.6 mm ID, 0.1% open area
D3	single nozzle, 5.1 mm ID, 0.1% open area
D4	perforated plate, 163 holes of 0.5 mm ID, 0.15% open area, equilateral triangle 1 cm apart
D5	perforated plate, 61 holes of 0.4 mm ID, 0.04% open area, 3 circular rings 1.5 cm apart
D6	perforated plate, 163 holes of 1.25 mm ID, 1.0% open area, equilateral triangle 1 cm apart

The tomographic attenuations were measured along several beam paths (projections) through the column from different coordinates. After a set of attenuation measurements was completed, the image of the attenuation of the mixture of phases in each pixel was reconstructed using the estimation−maximization (EM) algorithm.[5] The column cross-sectional domain is enclosed inside a square of 40 × 40 pixels. The EM algorithm has the following advantages: (1) it accounts for statistical variations associated with radiation measurements; (2) it readily incorporates nonuniform beam effects; and (3) it ensures that the final reconstruction will contain non-negative values.

3. Results and Discussions

This section consists of two parts: (1) the experimental results and their discussion, and (2) an analysis of the bubble formation and its flow regime in the sparger region based on the literature findings. Systematic experimental investigations of the sparger region are recommended, but, are not the focus of this work.

3.1. Effect of the Sparger on the Gas Holdup Radial Profiles Using the CT Technique. 3.1.1. The Axisymmetry of Gas Holdup Radial Profiles. To evaluate the symmetry of the time-averaged gas holdup cross-sectional distribution over the range of operating conditions used in this study measured by CT (results of these scans are not shown here, please refer to ref 26), an example is provided in Figure 3. This figure shows the radial variation of gas holdup in the four quadrants at three different pressures for perforated plate distributors (D4 and D6) and the single nozzle sparger (D3). Each point for each quadrant of Figure 3 was obtained by averaging the holdup of the arc of the pixels at a given dimensionless radius (r/R). It is noteworthy that there are more pixels near $r/R = 1$ than near the column center ($r/R = 0$). However, for both regions, the number of CT projections is the same, as discussed earlier. The CT projections are used to reconstruct the holdups in the pixels corresponding to the dimensionless radius indicated in Figure 3. Hence, in the region of the column center, where there are fewer pixels in the arc, more projections pass through these pixels, compared to the pixels of the arc near the wall region. One can notice that the differences in the radial gas holdup profiles of the four quadrants are within 5% of the overall azimuthal mean of the four quadrants taken together. The average of the four averaged data points of the four quadrants at a certain dimensionless radial location represents the mean gas holdup at that specific radial location. This gives the mean holdup profile. The upper and lower bounds to the mean are calculated as twice the standard deviation, where the standard deviation of the holdup at any radial location is obtained using these averaged data points of the four quadrants. Based on the findings (Figure 3, for example) and, for engineering purposes, one can conclude that the gas holdup distributions are azimuthally symmetric. It is noteworthy that there is an increase in the gas holdup in the central region of the column within the range of dimensionless radius from $r/R \approx 0.25$ to $r/R \approx 0$. It was later determined that this was due to an artifact in the inside structure of the source collimator, which provides different beam activity strength in the central region of the beam (which covers the central region of the column) than in other regions of the fan beam. Such a trend is clearly noticed in the other figures.

3.1.2. The Reproducibility of the CT Measurements. The reproducibility of the CT measurements for the gas holdup was also addressed in this study. Two different batches of tap water on three different days were used to assess the reproducibility of the CT measurements using the perforated plate distributor D4 (0.15% open area, $d_o = 0.5$ mm). The results shown in Figure 4 indicate good reproducibility. At atmospheric pressure, the bounds for the 95% confidence interval, consisting of two standard deviations on each side of the mean, are well within ±2% at every radial location except at the points close to the wall, which are within ±5%. For the higher pressure of 4 atm,

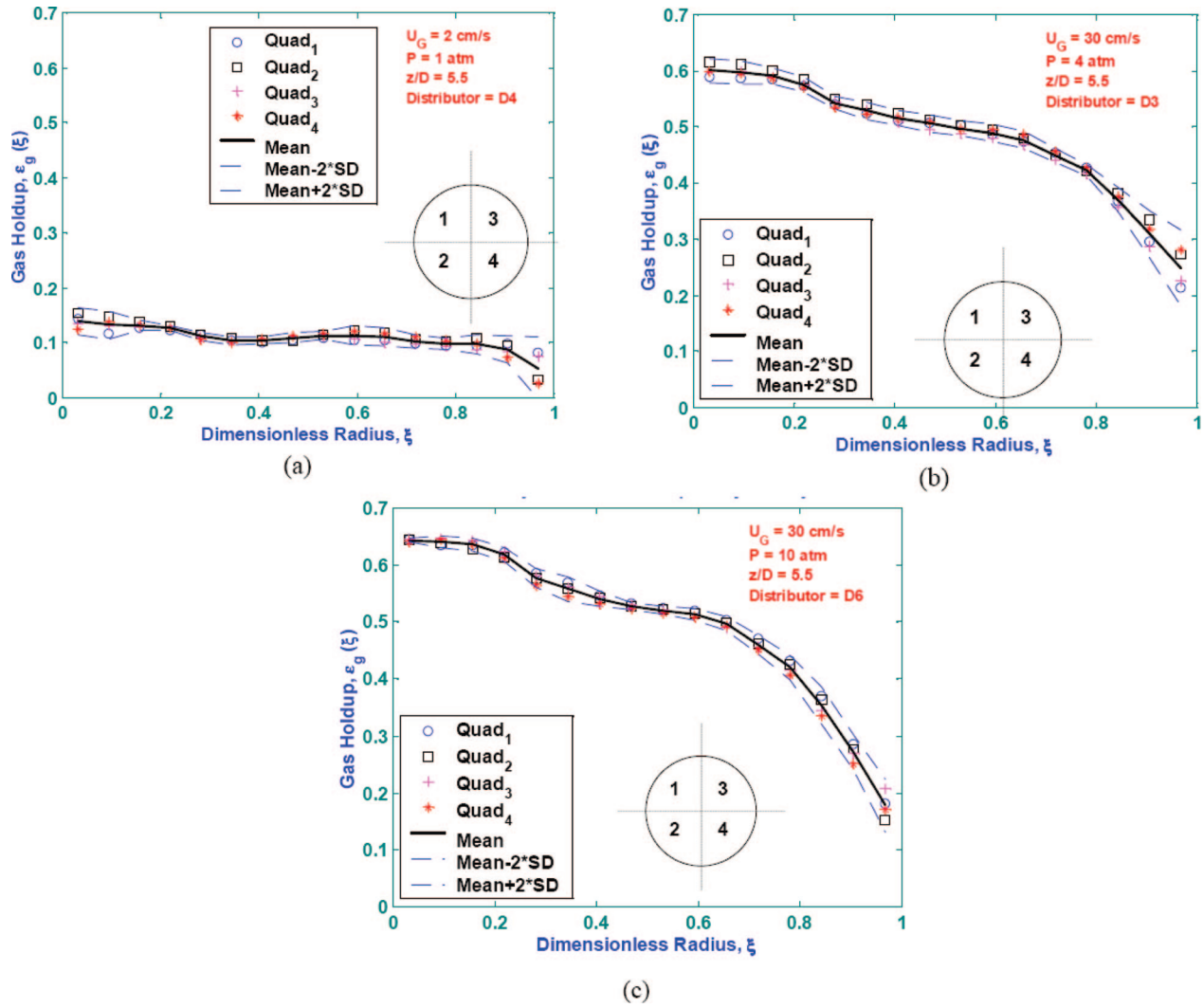

Figure 3. Radial gas holdup profiles in the four different quadrants of the cross-sectional gas holdup: (a) D4, $U_g = 2$ cm/s, $P = 1$ atm; (b) D3, $U_g = 30$ cm/s, $P = 4$ atm; and (c) D6, $U_g = 30$ cm/s, $P = 10$ atm.

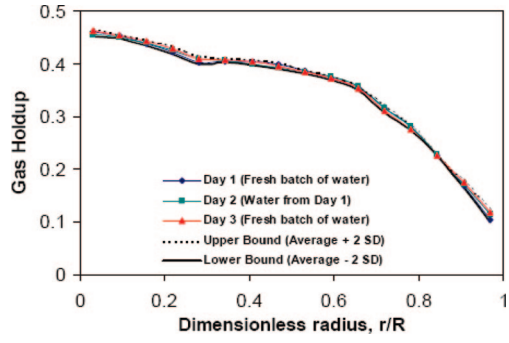

Figure 4. Reproducibility of the radial gas holdup profiles at superficial gas velocity of 30 cm/s at (a) $P = 1$ atm and (b) $P = 4$ atm, using two different batches of water on three different days, using a perforated plate distributor D4 (0.15% open area; $d_o = 0.5$ mm).

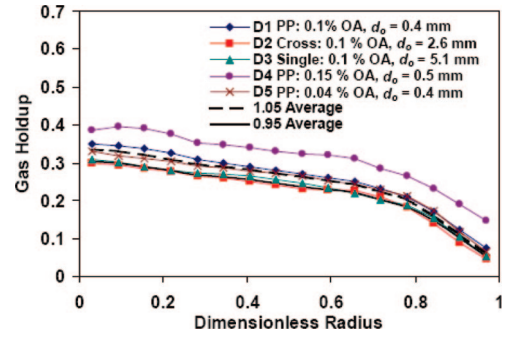

Figure 5. Effect of spargers at $U_g = 14$ cm/s at a scan level of $z/D = 5.5$ ($P = 1$ atm).

all data points in the radial gas holdup profiles are within ±4% of the average radial gas holdup profile. The standard deviation of the measured gas holdup at each dimensionless radial profile is estimated as outlined previously.

3.1.3. Time-Averaged Gas Holdup Radial Profile. Figures 5 and 6 show the radial gas holdup profiles, $\varepsilon_{gi}(r)$ for each distributor ($i = 1, 2, 3, 4, 5$ or 6; see Table 1 and Figure 2 taken at $z/D = 5.5$), for superficial gas velocities of 14 and 30 cm/s, respectively, at atmospheric pressure. The perforated plate distributor (D1), cross sparger (D2), and single nozzle (D3) have the same percentage of open area (POA). Therefore, to examine whether they produce similar holdup profiles at a given axial elevation z, the mean holdup profile of these distributors at each radial location is calculated as $\varepsilon_g(r, z) = \sum_{i=1}^{N} \varepsilon_{gi}(r, z)/N$ (where $j = 1, 2, 3$). The distributor effect is considered insignificant if $\varepsilon_{gi}(r,z)$ lies within the range from 0.95 $\varepsilon_g(r,z)$ to 1.05 $\varepsilon_g(r,z)$. This represents a narrow band around the mean (±5%). From Figure 5, it is evident that, at $U_g = 14$ cm/s, not all the distributors generate a gas holdup profile in that band. These differences are notable not only near the distributor zone (not

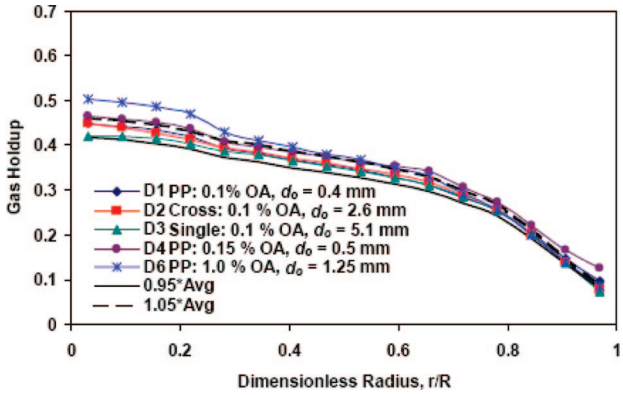

Figure 6. Effect of spargers at $U_g = 30$ cm/s at a scan level of $z/D = 5.5$ ($P = 1$ atm).

shown here; please refer to ref 26), but also throughout the column. There are differences in gas holdup profiles produced by different distributors at dimensionless radii $r/R < 0.8$ in the core of the column (see Figures 5 and 6).

Examination of Figure 5 reveals that, for a U_g value of 14 cm/s and at atmospheric pressure, the cross and single nozzle spargers produce the lowest radial gas holdup profile, whereas the perforated plate distributors produce higher holdups that are proportional to their POA. In other words, for the perforated plate distributors, the holdup is the largest for D4 (POA = 0.15), followed by D1 (POA = 0.1) and D5 (POA = 0.04). However, distributors D2 and D3, which are the cross and the single nozzle spargers, respectively, generate almost identical gas holdup profiles. The behavior of D2 and D3 is significantly different even from distributor D1, which has the same POA, but is a perforated plate. Kumar[5] also observed a similar trend in measured gas holdup profiles, using a slightly larger column (19 cm in diameter) with a perforated plate (166 holes of 0.33 mm ID, square pitch, POA = 0.05), bubble cap, and cone distributor. One possible explanation for the observed differences may lie in the bubble formation regimes of the different spargers. Because of the significantly stronger jetting/dispersed jetting mode of gas introduction by spargers D2 and D3, as will be discussed later in section 3.2, it is likely that a stable bubble structure, such as that produced by perforated plates, cannot be maintained. Hence, early transition to the churn-turbulent flow regime occurs. It is likely, then, that the perforated plate distributors induce a very stable bubble structure in the column that suppresses the coalescence of bubbles and leads to higher gas holdups. These observations indicate that the transition to churn-turbulent flow is indeed dependent on the sparger type, along with the physical properties of the system used, and few of the previously reported studies seem to consider this effect. Xue et al.,[27] Xue,[28] and Xue et al.[29,30] have addressed the investigation of bubble dynamics using a four-point probe, whereas Shaikh and Al-Dahhan[31] and Shaikh[32] have investigated the flow regime transition in bubble columns. These studies confirm the findings and the analysis previously obtained.

Remember that perforated plates are rarely used for industrial systems, with spargers similar to D2 and D3 being preferred. Therefore, it can be said that, for industrially important spargers, the effect of sparger design can be considered negligible for superficial gas velocities exceeding 14 cm/s at $P = 1$ atm.

As mentioned earlier, at $P = 1$ atm and $U_g = 14$ cm/s, when one compares the radial gas holdup distributions for the perforated plate distributors (D1, POA = 0.1; D4, POA = 0.15; D5, POA = 0.04), one sees that the gas holdup obtained using D4 is systematically higher than that for D1 at all radial locations (see Figure 5). The reason for this could be the larger size of the orifice holes for distributor D4 (0.5 mm), compared to that of D1 (0.4 mm). Therefore, despite the same distribution of orifices for these two spargers, the same bubble number density (per unit sparger cross section) with larger bubble diameter will result in greater gas holdup for distributor D4. A larger orifice diameter implies a lower orifice velocity; hence, slightly larger bubbles are formed with lower ejection velocity and a lower frequency of bubbling. Also, with similar bubble number density, larger bubbles would produce greater hindrance to the rise of individual bubbles, implying a larger holdup. If this distribution of bubbles does not undergo coalescence as the bubble swarm rises, a larger gas holdup for D4 could be maintained along the entire column length, compared to the gas holdup obtained using D1. These findings have been also reported,[27−30] as mentioned previously.

The previous observations regarding the gas holdup distributions obtained using spargers D1 and D4 are contrary to the findings of Tsuchiya and Nakanishi,[13] who concluded that the overall mean gas holdup decreases as the orifice diameter increases, when keeping the number of holes on the perforated plate fixed. However, their measurements were made in a very tall column of 14.8 cm ID and 8.0 m height, resulting in $L/D = 55$ and allowing larger bubbles to form as a result of enhanced coalescence (an air−water system (i.e., coalescing system) was used in the study). The holdup obtained with D5 is lower than that obtained with D1, probably due to a lower POA; however, there is no clear trend in the differences at various radial locations.

Nevertheless, considering all the spargers evaluated in this study, sparger design does seem to have some influence on gas holdup, even under operating conditions that are normally taken to be in the churn-turbulent regime, such as $U_g = 14$ cm/s at $P = 1$ atm.[32] However, as shown in Figure 6, deep in the churn-turbulent regime, at a superficial gas velocity of 30 cm/s, the sparger's effect on holdup distribution is small but not insignificant, which is in agreement with other reported studies.[7,11,13]

From Figure 6, one observes that gas holdup values are higher and that the difference in gas holdups for the different spargers is much narrower than the results at $U_g = 14$ cm/s. One also sees that spargers D4 and D6, which exhibit the bubbling regime of bubble formation, produce higher gas holdups in the center of the column, while the single nozzle sparger (D3) produces the lowest. This implies that, for the perforated plate spargers, the bubble number density of the smaller bubbles is larger in the column center (moreso for D6, followed by D4, then D1), compared to the cross and single nozzle spargers.[28] Therefore, although it might be tempting to conclude that, for practical engineering purposes, the effect of distributors on gas holdup is insignificant at $U_g = 30$ cm/s and $P = 1$ atm, the CT measurements from this study indicate that the detected differences are small but do exceed the previously defined band of reproducibility of results for one sparger. The distributor's effect on gas holdup profile remains small, even when the open area of the distributors is changed from 0.1% (perforated plate D1, cross sparger D2, single nozzle D3) to 1.0% (perforated plate D6). Compared to the holdups for D1, D2, and D3 with 0.1% open area, only slightly higher holdups at $r/R > 0.9$ were observed for the perforated plate distributor D4 with 0.15% open area, and at $r/R < 0.2$ for the perforated plate distributor D6 with 1.0% open area. Therefore, at atmospheric pressure and deep in the churn-turbulent regime for tall columns, it may be reasonable to assume insignificant distributor effects on gas holdup.

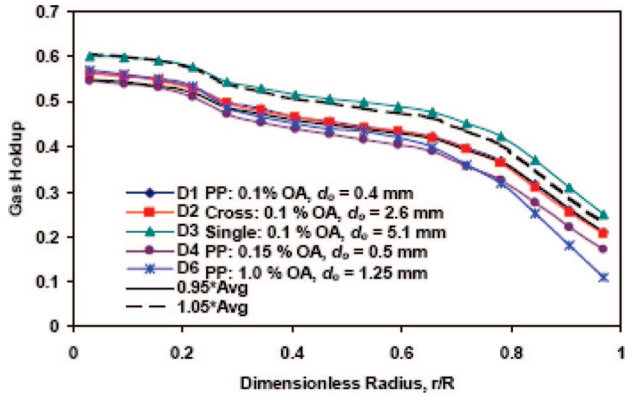

Figure 7. Effect of spargers at $U_g = 30$ cm/s at a scan level of $z/D = 5.5$ ($P = 4$ atm).

The results presented so far were for different U_g values and spargers at atmospheric pressure. In addition, the effect of spargers on gas holdup radial profiles at a higher operating pressure was examined. Figure 7 displays the radial gas holdup profiles for distributors D1, D2, D3, D4, and D6 measured at a superficial gas velocity of 30 cm/s at $z/D = 5.5$ at $P = 4$ atm. As shown in Figure 7, the radial gas holdup profiles for perforated plate distributor D1 and cross sparger D2 fall within the 10% band around the mean, whereas the holdup profiles generated by D3 (single nozzle of 0.1% porosity) and D6 (perforated plate of 1% porosity) lie above and below the 10% band, respectively.

If one considers all the distributors other than D3 (single nozzle), at $P = 4$ atm and $U_g = 30$ cm/s, one can conclude that there is not a significant distributor effect on radial gas holdup profile, except near the column walls. Figure 7 also shows that the radial gas holdup exhibited using D3 (single nozzle) is comparatively much higher than for the rest of the distributors.

This higher holdup could be explained based on the studies conducted by Kling[33] and La Nauze and Harris,[34] who used nozzles of various orifice diameters. They reported that, when the pressure is increased, the gas jet produced by the nozzle disperses, breaks up more rapidly, and forms more-numerous small bubbles. In this case, the level of liquid turbulence generated using a single nozzle might be so much greater than the turbulence generated by the perforated plate and cross distributors, that, as a result, the gas holdup increases substantially for the single nozzle sparger. Further investigation is recommended at a range of operating pressures to fully characterize the effect of pressure along with different sparger designs.

3.1.4. Axial Variation of Gas Holdup Radial Profile. Figures 8 and 9 show the axial variation of the radial holdup profile for the perforated plate distributor D1 and for the single nozzle sparger D3 at a superficial gas velocity $U_g = 14$ cm/s and atmospheric pressure, respectively. From Figure 8, which is for a uniform perforated plate distributor D1, one can clearly see a noticeable axial variation of gas holdup. One also observes a consistent trend for this perforated plate distributor (D1), where the gas holdup uniformly decreases with height. This implies that, at this superficial gas velocity, the primary bubble size at the distributor is smaller than the secondary (stable) bubble size.[8] Similar conclusions regarding the axial variation of the radial gas holdup profiles are obtained for the other perforated plate distributors D4 and D5. For a single nozzle distributor D3, as displayed in Figure 9, there is a relatively small but finite axial variation of the radial gas holdup profile. The figure shows that gas holdup marginally increases with height, which implies that

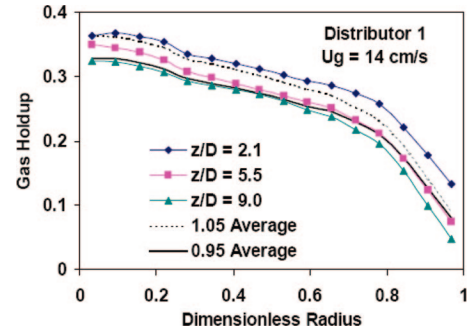

Figure 8. Axial variation of gas holdup for perforated plate distributor D1 (0.1% open area; $d_o = 0.4$ mm) at $U_g = 14$ cm/s ($P = 1$ atm).

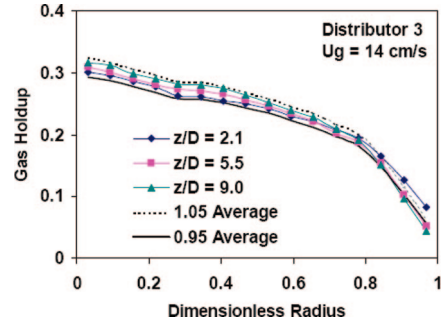

Figure 9. Axial variation of gas holdup for single nozzle sparger D3 (0.1% open area; $d_o = 5.1$ mm) at $U_g = 14$ cm/s ($P = 1$ atm).

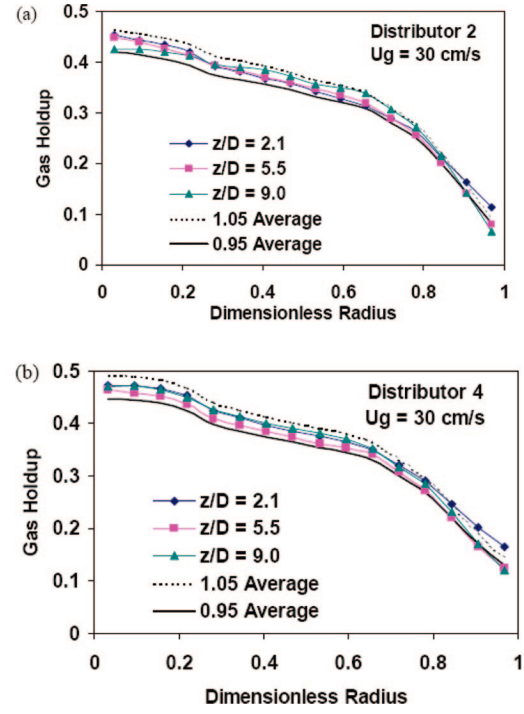

Figure 10. Axial variation of gas holdup for (a) cross sparger D2 (0.1% open area; $d_o = 2.6$ mm) and (b) perforated plate D4 (0.15% open area; $d_o = 0.5$ mm) at $U_g = 30$ cm/s ($P = 1$ atm).

the average bubble size at the sparger is slightly larger than the equilibrium bubble diameter. These findings are in agreement with studies of Shollenberger et al.[35] The same observation holds for the cross sparger (D2) and can be explained in terms of the stable bubble size, which is attained relatively close to the sparger, implying that the sparger zone for these two distributors is confined to less than two column diameters.

Table 2. Flow Conditions at the Orifice[a]

range of N_c	flow condition at the orifice
$N_c < 1$	constant flow
$1 < N_c < 9$	intermediate condition
$9 < N_c$	constant pressure

[a] From Ong.[26]

Table 3. Formation of Bubbles at the Orifice[a]

range of N_w	small, uniform bubbles are formed
$2.4(N_c - 1) < N_w < 16$	bubble volume increases with N_w
$16 < N_w$	bubbles break down after detachment at the orifice and distribution of bubble volumes is produced

[a] From Ong.[26]

As shown in Figure 10 for D2 (cross sparger) and D4 (perforated plate distributor), at $U_g = 30$ cm/s and at $P = 1$ atm, the radial gas holdup profiles for all distributors investigated are not a function of axial position (except for points at $r/R > 0.85$ at $z/D = 2.1$). This finding implies that the entry region is confined to about two column diameters, which is consistent with the findings of Shollenberger et al.[35]

3.2. Analysis of the Literature on Bubble Formation and Flow Regimes at the Sparger Region. Many studies have addressed bubble formation from a single orifice submerged in liquids at atmospheric pressure (e.g., refs 36−39) and at high pressure (see refs 34, 40−42). It has been understood that the formation of bubbles at submerged orifices is influenced by many factors, such as the orifice diameter, superficial gas velocity through the orifice, liquid density, liquid viscosity, surface tension, orifice material, and gravitational acceleration. In addition, each bubble is acted upon by numerous forces that affect its motion and shape.[15,43]

Tadaki and Maeda[44] proposed the following dimensionless numbers to characterize bubble formation:

$$N_o = \frac{4V_{ch}g\rho_l}{\pi d_g^{\,2} p_h} \tag{1}$$

$$N_w = \mathrm{Bo}Fr_o^{\,0.5} \tag{2}$$

where V_{ch} is the chamber volume feeding the orifice, p_h the hydrostatic pressure at the orifice plate, Bo the bond number ($\mathrm{Bo} = \rho g d_o/\sigma$), and Fr_o the Froude number at the orifice ($Fr_o = u_o^2/(gd_o)$). Based on these two numbers (N_c and N_w), the flow conditions and formation of bubbles at the orifice are summarized in Tables 2 and 3.[26] Details on the bubble formation and detachment from a single orifice, as well as its rise velocity, have been discussed and analyzed elsewhere.[41,45−48] However, bubble formation from multiple orifices or distributors of different designs is still not well-understood. Degaleesan[2] reviewed different regimes of bubble formation at the orifice for multiple-orifice spargers, along with the correlations used to obtain the initial bubble diameter (refer to Table 4).

Because the expressions for the dimensionless capacitance (N_c) and gas flow rate numbers (N_w) (refer to eqs 1 and 2) are based on a single orifice submerged in liquid, the estimation of these dimensionless numbers for all the six spargers used in this work required certain assumptions, which are discussed subsequently. As can be seen from eq 1, the dimensionless capacitance number requires the gas chamber volume as input. In this study, the chamber volume per unit orifice is evaluated as V_{ch}/N_o (N_o represents the number of orifices on a sparger) and is subsequently used instead of the total chamber volume to calculate N_c. The total chamber volume (V_{ch}) is 1460 cm^3.

Table 4. Initial Bubble Size Correlations[a]

regime	bubble size equation	reference
single bubble ($Re_o = \rho_g u_o d_o/\mu_o) \le 200$	$d_b = \left[\frac{6\sigma d_o}{(\rho_l - \rho_g)g}\right]^{1/3}$	Azbel[45]
intermediate bubble	$d_b = 0.19 d_o^{0.48} Re_o^{0.32}$ (where d_b and d_o are given in inches)	Leibson et al.[46]
jetting criterion $200 < Re_o < 2100$	$u_\bigcirc > u_{o,crit}$ $\frac{u_{o,crit}\sqrt{\rho_g}}{[\sigma(\rho_l - \rho_g)]^{1/4}} = 1.3\left[\frac{g^2\sigma}{(\rho_l - \rho_g)d_o^{\,2}}\right]^{1/12}$	Azbel[45]
jetting ($Re_o > 2100$)	$d_b = 0.28 Re_o^{-0.05}$ (where d_b is given in inches)	Leibson et al.[46]

[a] From Degaleesan.[2]

Table 5 displays N_c and N_w, each as a function of pressure, and U_g for the six distributors used in this study.[26]

From column 6 of Table 5, it can be seen that constant flow conditions prevail at the orifice ($N_c < 1$) if the orifice diameter is close to or above 1.25 mm at a pressure of 10 atm. The other noteworthy observation based on the *N*c values from Table 5 is that, except for distributor D5, which was operated under atmospheric conditions, no distributor operated at $N_c > 9$. This implies that the bubble volume at the sparger is dependent on the chamber volume. Only for distributor D5, bubbles are formed under constant pressure conditions. The other factor characterizing the formation of bubbles at the orifice is the dimensionless gas flow rate number, N_w. As presented earlier, at $N_w > 16$, the bubbles formed at the sparger break down after detachment at the orifice, resulting in a distribution of bubble sizes. Therefore, it is interesting to determine the superficial gas velocity at which N_w value is >16 for the six distributors used in the study. This can be readily inferred from Figure 11, where the variation of N_w with U_g is presented, as well as from Table 5. Figure 11 shows that the superficial gas velocity at which N_w becomes equal to 16 is the smallest for the single nozzle distributor D3, followed by the cross sparger D2 and then the perforated plates in increasing order of the POA (D5, D1, D4, D6). It is also noteworthy that, for the same number of orifices (D1, D4, and D6), increasing the size of the orifice increases the transition superficial gas velocity, which implies that, for the same U_g and same number of orifices, an increase in orifice diameter leads to more-stabilized bubble detachment with lower subsequent bubble breakup. It should be further noted that the gas density does not appear anywhere in the expression for N_w, implying that it is independent of operating pressure. In addition, irrespective of the type of distributor, the superficial gas velocity at which N_w exceeds 16 is <10 cm/s. Therefore, based on this criterion, the bubble formation at the sparger for the majority of the experiments performed in this study results in a distribution of bubble sizes. This can also be seen from Table 5, where the values of N_w for most spargers and operating conditions are >16, implying that a broad spectrum of bubble sizes are formed at the sparger. Although characterizing the bubble size distribution in the sparger region and in the fully developed region is important, this task is not part of this study. Separate studies in our laboratory have tackled this issue, and the results have been reported.[27−30] Figure 12 displays the assessment of the sparger region flow regime (bubbling, jetting or dispersed jetting) for different distributors under different operating conditions, based on the correlation of Idogawa et al.[40] (Refer to the equations given in Figure 12.)

Table 6 lists the various operating conditions that correspond to the different sparger region flow regimes shown in Figure

Table 5. N_c and N_w Values, as a Function of P for All the Distributors Studied[a]

P (atm)	U_g (m/s)	u_o (m/s)	H_s (m)	N_c	N_w	Bubble Formation Criterion based on N_c	Bubble Formation Criterion based on N_w[b]
			D1 (0.1%, 163 Orifices of 0.4 mm)				
1	0.14	140	1.49	6.89	48.7	intermediate	3
1	0.3	301	1.43	6.89	104	intermediate	3
1	0.45	332[c]	1.35	6.89	115	intermediate	3
4	0.3	300	1.32	1.72	104	intermediate	3
			D2 (0.1%, 4 Orifices of 2.6 mm)				
1	0.14	135	1.53	6.64	779	intermediate	3
1	0.3	289	1.43	6.64	1670	intermediate	3
4	0.3	289	1.32	1.66	1670	intermediate	3
			D3 (0.1%, 1 Orifice of 5.1 mm)				
1	0.14	140	1.52	6.91	2230	intermediate	3
1	0.3	301	1.43	6.91	4770	intermediate	3
4	0.3	301	1.27	1.73	4770	intermediate	3
			D4 (0.15%, 163 Orifices of 0.5 mm)				
1	0.02	12.8	1.64	4.41	6.23	intermediate	1
1	0.08	51.2	1.38	4.41	24.9	intermediate	3
1	0.14	89.6	1.42	4.41	43.6	intermediate	3
1	0.3	192	1.40	4.41	93.4	intermediate	3
1	0.45	288	1.33	4.41	93.4	intermediate	3
1	0.6	332[c]	1.28	4.41	161	intermediate	3
4	0.02	12.8	1.65	1.10	6.23	intermediate	2
4	0.08	51.2	1.37	1.10	24.9	intermediate	3
4	0.14	89.6	1.45	1.10	43.6	intermediate	3
4	0.3	192	1.35	1.10	93.4	intermediate	3
4	0.45	288	1.28	1.10	140	intermediate	3
10	0.02	12.8	1.64	0.44	6.23	constant flow	2
10	0.08	51.2	1.39	0.44	24.9	constant flow	3
10	0.14	89.6	1.32	0.44	43.6	constant flow	3
			D5 (0.04%, 61 Orifices of 0.4 mm)				
1	0.14	332[c]	1.49	18.4	116	constant pressure	3
			D6 (1%, 163 Orifices of 1.25 mm)				
1	0.3	30.7	1.41	0.705	59.1	constant flow	3
4	0.3	30.7	1.36	0.176	59.1	constant flow	3
10	0.3	30.7	1.27	0.071	59.1	constant flow	3

[a] Data taken from Ong.[26] [b] Legend: 1, single uniformed bubbles are formed; 2, bubble volume increases with N_w; and 3, bubbles break down after detachment at the orifice and a distribution of bubble volumes is produced. [c] Sonic velocity at 70 °F (298 K) = 332 m/s. Choked flow occurs when the sonic velocity has been attained.

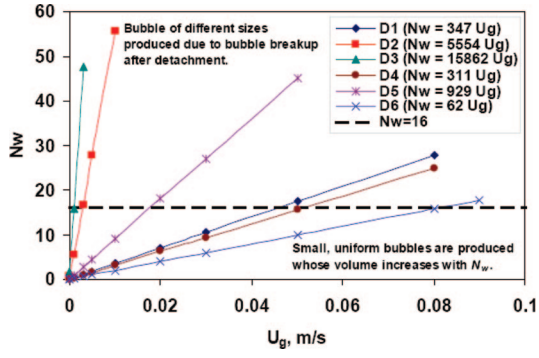

Figure 11. Dimensionless gas flow rate versus superficial gas velocity for all the distributors studied: $N_w = BoFr_o^{0.5}$.

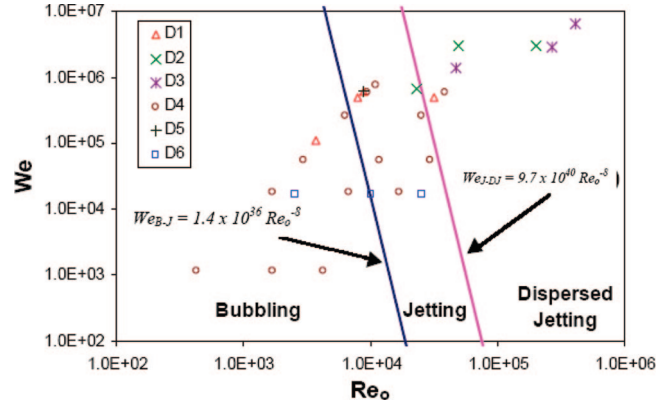

Figure 12. Plot of the Weber number ($We = \rho_l u_o^2 d_o/\sigma$) versus the Reynolds number ($Re = \rho_g u_o d_o/\mu_g$ for different distributors under different operating conditions. (Equations obtained from Idogawa et al.[40])

12. As shown in Table 6, beyond a superficial gas velocity of 14 cm/s, the flow is either in the jetting or dispersed jetting regime for most operating conditions. The only exceptions occur when using the perforated plate distributors D4 (0.15% open area) and D6 (1.0% open area) operating at a pressure of 1 atm and superficial gas velocity of 30 cm/s (refer to Table 6). These two distributors have a larger POA than the perforated plate distributor D1 (0.1%). Hence, the orifice velocity using the perforated plate distributor D1 is higher, compared to the other two distributors. In fact, the perforated plate distributor D1 was designed in such a way that the orifice velocity approaches the sonic velocity. Another important observation to make from Table 6 is that, for distributor D4, the onset of jetting is expedited with pressure, i.e., the jetting regime is attained at a lower superficial gas velocity with increasing pressure. Hence, this indicates that the bubbling regime is generally favored by flow through perforated plate distributors of sufficient open area and at lower operating pressures.

Table 6. Bubble Formation Regimes under Various Operating Conditions[a]

P (atm)	U_g (m/s)	u_o (m/s)	Re_o	We	Bubble Formation Regime from Idogawa et al.[40]	Bubble Formation Regime from Leibson et al.[46]
			D1 (0.1%, 163 Orifices of 0.4 mm)			
1	0.14	140	3710	109000	bubbling	jetting
1	0.3	301	7940	499000	jetting	jetting
1	0.45	332[b]	8790	611000	jetting	jetting
4	0.3	301	31800	499000	dispersed jetting	jetting
			D2 (0.1%, 4 Orifices of 2.6 mm)			
1	0.14	135	23200	6580000	jetting	jetting
1	0.3	289	49800	3020000	dispersed jetting	jetting
4	0.3	289	199000	3020000	dispersed jetting	jetting
			D3 (0.1%, 1 Orifice of 5.1 mm)			
1	0.14	140	47400	1390000	dispersed jetting	jetting
1	0.3	301	102000	6400000	dispersed jetting	jetting
4	0.3	301	406000	6400000	dispersed jetting	jetting
			D4 (0.15%, 163 Orifices of 0.5 mm)			
1	0.02	12.8	424	1140	bubbling	intermediate
1	0.08	51.2	1700	18200	bubbling	intermediate
1	0.14	89.6	2970	55700	bubbling	jetting
1	0.3	192	6350	256000	bubbling	jetting
1	0.45	288	9530	575000	jetting	jetting
1	0.6	332[b]	11000	764000	jetting	jetting
4	0.02	12.8	1700	1140	bubbling	intermediate
4	0.08	51.2	6780	18200	bubbling	jetting
4	0.14	89.6	11800	55700	jetting	jetting
4	0.3	192	25400	256000	jetting	jetting
4	0.45	288	38100	575000	dispersed jetting	jetting
10	0.02	12.8	4240	1140	bubbling	jetting
10	0.08	51.2	16900	18200	jetting	jetting
10	0.14	89.6	29700	55700	jetting	jetting
			D5 (0.04%, 61 Orifices of 0.4 mm)			
1	0.14	332[b]	8790	611000	jetting	jetting
			D6 (1%, 163 Orifices of 1.25 mm)			
10	0.3	30.7	25400	16400	jetting	jetting
4	0.3	30.7	10200	16400	jetting	jetting
10	0.3	30.7	25400	16400	jetting	jetting

[a] Data taken from Ong.[26] [b] Sonic velocity at 70 °F (298 K) = 332 m/s. Choked flow occurs when the sonic velocity has been attained.

4. Concluding Remarks

This study used γ-ray computed tomography (CT) technique to investigate the effect of sparger design on the gas holdup radial profiles in a bubble column. Six different spargers were used at selected operating conditions.

The main findings of the current study can be summarized as follows:

(1) For all the sparger configurations used, the gas holdup always increased as the superficial gas velocity increased. The holdup also increased as the pressure increased up to 4 atm, although this was observed only in churn-turbulent flow at higher superficial gas velocities.

(2) The assumption of axisymmetry in time-averaged gas holdup distribution was valid at both atmospheric pressure and the higher pressure that was used.

(3) At both $U_g = 14$ and 30 cm/s, there were significant differences in the gas holdup profiles produced by different distributors at dimensionless radii of <0.8 in the core of the column.

(4) The cross and single nozzle spargers (D2 and D3, respectively), which are preferred in industrial applications, produced almost identical gas holdup profiles.

(5) The lowest radial gas holdup profile was obtained with D2 and D3 spargers, whereas the perforated plate (D1) produced a higher gas holdup, although it has the same POA as D2 and D3. This might be due to the fact that such a perforated arrangement suppresses the bubbles' coalescence, yielding a higher gas holdup.

(6) At higher pressure (4 atm), all studied distributors (other than the single nozzle (D3)) had no significant effect on gas holdup except near the wall. D3 produced a much higher gas holdup.

In summary, while the effect of distributors on gas holdup deep in the churn-turbulent regime under the studied conditions is small, the effect should not be entirely ignored during reactor design and scaleup, especially when a fast chemistry may be involved where a majority of the reaction happens close to the distributor. However, extended investigations should be conducted to systematically cover the study of bubble dynamics in the sparger region besides the fully developed flow region, using conditions and gas−liquid systems of interest to industrial applications.

Acknowledgment

The authors would like to acknowledge the financial support provided by the Department of Energy through Air Products and Chemicals, Inc., (under DOE Contract No. FC 22 95 PC 95051), and specially thank Dr. Kemoun Abdenour for his assistance with the experimental setup.

Nomenclature

Abbreviations

Bo = bond number
CT = computed tomography
EM = estimation-maximization
POA = percentage open area

Variables

d_o = sparger orifice diameter (mm)
H_s = dispersed height
L = column height
L_s = dispersed height
N = number of radial locations
N_c = capacitance number
N_w = gas flow rate number
P = operating pressure (MPa)
P_o = a certain constant pressure (MPa)
p_h = hydrostatic pressure at the orifice plate
Q_g = gas flow rate (cm^3/s)
r = radial position in the column (cm)
R = column radius (cm)
Re_o = orifice Reynolds number based on gas properties
U_g = superficial gas velocity (cm/s)
u_o = centerline interstitial liquid velocity (cm/s)
V_{ch} = chamber volume (cm^3/s)
$We_{J\text{-}DJ}$ = Weber number for the jetting/dispersed jetting transition
$We_{B\text{-}J}$ = Weber number for the bubbling/jetting transition
z = axial position in the column (cm)
ρ_l = liquid density
ρ_g = gas density
ε_g = gas holdup
ε_{gi} = radial gas holdup profile
σ = surface tension (mN/m)

Literature Cited

(1) Jamialahmadi, M.; Muller-Steinhagen, H.; Sarrafi, A.; Smith, J. M. Studies of gas holdup in bubble column reactors. *Chem. Eng. Technol.* **2000**, *23* (10), 919–921.

(2) Degaleesan, S., Turbulence and Liquid Mixing in Bubble Columns, D.Sc. Thesis, Washington University, St. Louis, MO, 1997.

(3) Gupta, P. Churn-Turbulent Bubble Columns−Experiments and Modeling, D.Sc. Thesis, Washington University, St. Louis, MO, 2002.

(4) Gupta, P.; Ong, B.; Al-Dahhan, M. H.; Dudukovic, M. P.; Toseland, B. A. Hydrodynamics of Churn-Turbulent Bubble Columns: Gas−Liquid Recirculation and Mechanistic Modeling. *Catal. Today* **2001**, *64* (3−4), 253–269.

(5) Kumar, S. B. Computed Tomographic Measurements of Void Fraction and Modeling of the Flow in Bubble Columns, Ph.D. Thesis, Washington University, St. Louis, MO, 1994.

(6) Hebrard, G.; Bastoul, D.; Roustan, M. Influence of the Gas Sparger on the Hydrodynamic Behavior of Bubble Columns. *Trans. Inst. Chem. Eng. A* **1996**, *74*, 406–414.

(7) Krishna, R.; Ellenberger, J. Gas Holdup in Bubble Column Reactors Operating in the Churn-Turbulent Flow Regime. *AIChE J.* **1996**, *42* (9), 2627–2634.

(8) Joshi, J. B.; Parasu Veera, U.; Prasad, Ch. V.; Phanikumar, D. V.; Deshphande, N. S.; Thakre, S. S.; Thorat, B. N. Gas Holdup Structure in Bubble Column Reactors. *PINSA* **1998**, *64A* (14), 441–567.

(9) Freedman, W.; Davidson, J. F. Hold-up and Liquid Circulation in Bubble Columns. *Trans. Inst. Chem. Eng.* **1969**, *47*, T251−T262.

(10) Ueyama, K.; Morooka, S.; Koide, K.; Kaji, H.; Miyauchi, T. Behavior of Gas Bubbles in Bubble Columns. *Ind. Eng. Chem. Process Des. Dev.* **1980**, *19* (4), 592–599.

(11) Mikkilineni, S.; Knickle, H. N. The Effect of Gas Distributors on Holdup and Flow Pattern in Bubble Column. In *Part. Multiphase Processes: Proceedings of the International Symposium and Workshop*, 1987; Vol. 3, pp 127−145.

(12) Rivas, O.; Bresolin, G. A.; Estevez, L. A.; Santamaria, X.; Cavicchioli, I. Effect of Gas Distribution on the Fluid Dynamics of Three-Phase Bubble Columns. *Rev. Tec. INTEVEP* **1987**, *7* (2), 97–102.

(13) Tsuchiya, K.; Nakanishi, O. Gas Holdup Behavior in a Tall Bubble Column with Perforated Plate Distributors. *Chem. Eng. Sci.* **1992**, *47*, 13–14.

(14) George, D. L.; Shollenberger, K. A.; Torczynski, J. R. Sparger Effects on Gas Volume Fraction Distributions in Vertical Bubble Column Flows as Measured by Gamma-Densitometry Tomography. In *Proceedings of FEDSM'00*, ASME Fluids Engineering Division Summer Meeting, 2000; pp 1−8.

(15) Luo, X.; Lee, D. J.; Lau, R.; Yang, G. Q.; Fan, L. S. Maximum Stable Bubble Size and Gas Holdup in High-Pressure Slurry Bubble Columns. *AIChE J.* **1999**, *45* (4), 665–680.

(16) Hills, J. H. Radial Non-Uniformity of Velocity and Voidage in a Bubble Column. *Trans. Inst. Chem. Eng.* **1974**, *52*, 1–9.

(17) Idogawa, K.; Ikeda, K.; Fukuda, T.; Morooka, S. Behavior of Bubbles of the Air−Water System in a Column Under High Pressure for Air−Water System. *Kagaku Kogaku Ronbunshu* **1985**, *11* (3), 253–258.

(18) Menzel, T.; Onken, U.; Wein, O. Deterministic and Stochastic Components of the Liquid Velocity in Gas−Liquid Reactors. *DECHEMA Monogr.* **1989**, *120*, 307–325.

(19) Yao, B. P.; Zheng, C.; Gasche, H. E.; Hofmann, H. Bubble Behavior and Flow Structure of Bubble Columns. *Chem. Eng. Process.* **1991**, *29*, 65–75.

(20) Chen, W.; Hasegawa, T.; Tsutsumi, A.; Otawara, K. Scale-up effects on the time-averaged and dynamic behavior in bubble column reactors. *Chem. Eng. Sci.* **2001**, *56*, 6149–6155.

(21) Kumar, S. B.; Moslemian, D.; Dudukovic, M. P. A γ-Ray Tomographic Scanner for Imaging Voidage Distribution in Two-Phase Flow Systems. *Flow Meas. Instrum.* **1995**, *6* (1), 61–73.

(22) Kumar, S. B.; Moslemian, D.; Dudukovic, M. P. Gas Holdup Measurements in Bubble Columns Using Computed Tomography. *AIChE J.* **1997**, *43* (6), 1414–1425.

(23) Chen, J.; Gupta, P.; Degaleesan, S.; Al-Dahhan, M. H.; Dudukovic, M. P.; Toseland, B. A. Gas Holdup Distribution in Large Diameter Bubble Columns Measured by Computed Tomography. *Flow Meas. Instrum.* **1998**, *9*, 91–101.

(24) Kemoun, A.; Ong, B. C.; Gupta, P.; Al-Dahhan, M. H.; Dudukovic, M. P. Gas Holdup in Bubble Columns at Elevated Pressure via Computed Tomography. *Int. J. Multiphase Flows* **2001**, *27* (5), 929–946.

(25) Rados, N., Slurry Bubble Columns Hydrodynamics, D.Sc. Thesis, Washington University, St. Louis, MO, 2003.

(26) Ong, B. C., Experimental Investigation of Bubble Column Hydrodynamics−Effect of Elevated Pressure and Superficial Gas Velocity, D.Sc. Thesis, Washington University, St. Louis, MO, 2003.

(27) Xue, J.; Al-Dahhan, M.; Duduković, M. P.; Mudde, R. F. Bubble dynamics measurements using four-point optical probe. *Can. J. Chem. Eng.* **2003**, *81*, 375–381.

(28) Xue, J., Bubble velocity, size and interfacial area measurements in bubble columns, D.Sc. Thesis, Washington University, St. Louis, MO, 2004.

(29) Xue, Junli; Al-Dahhan, Muthanna; Dudukovic, M. P.; Mudde, R. F. Four-point optical probe for measurement of bubble dynamics: Validation of the technique. *Flow Meas. Instrum.* **2008**, *19* (5), 293–300.

(30) Xue, J.; Al-Dahhan, M.; Duduković, M., P.; Mudde, R., F. Bubble velocity, size, and interfacial area measurements in a bubble column by four-point optical probe. *AIChE J.* **2008**, *54* (2), 350–363.

(31) Shaikh, A.; Al-Dahhan, M. A review on flow regime transition in bubble columns. *Int. J. Chem. Reactor Eng.* **2007**, *5*.

(32) Shaikh, A., Bubble and Slurry Bubble Column Reactors: Mixing, Flow Regime Transition and Scale Up, D.Sc. Thesis, Washington University, St. Louis, MO, 2007.

(33) Kling, G. Über die Dynamik der Blasenbildung Beim Begasen von Flüssigkeiten Unter Druck. *Int. J. Heat Mass Transfer* **1962**, *5*, 211–223.

(34) LaNauze, R. D.; Harris, I. J. Gas Bubble Formation at Elevated System Pressures. *Trans. Inst. Chem. Eng.* **1974**, *52* (4), 337–348.

(35) Shollenberger, K. A.; George, D. L.; Torczynski, J. R. Effect of Liquid Viscosity on the Development of Gas Volume Fraction Profiles in Vertical Bubble Column Flows. In *Proceedings of the 4th International Conference on Multiphase Flow*, 2000; pp 1−12.

(36) Tsuge, H.; Hibino, S. Bubble Formation from an Orifice Submerged in Liquids. *Chem. Eng. Commun.* **1983**, *22*, 63–79.

(37) Snabre, P.; Magnifotcham, F. I. Formation and Rise of a Bubble Stream in a Viscous Liquid. *Eur. Phys. J. B* **1998**, *4*, 369–377.

(38) Terasaka, K; Hieda, Y.; Tsuge, H. SO_2 Bubble Formation from an Orifice Submerged in Water. *J. Chem. Eng. Jpn.* **1999**, *32* (4), 472–479.

(39) Hsu, S. H.; Lee, W. H.; Yang, Y. M.; Chang, C. H.; Maa, J. R. Bubble Formation at an Orifice in Surfactant Solutions Under Constant-Flow Conditions. *Ind. Eng. Chem. Res.* **2000**, *39*, 1473–1479.

(40) Idogawa, K.; Ikeda, K.; Fukuda, T.; Morooka, S. Formation and Flow of Gas Bubbles in a Pressurized Bubble Column with a Single Orifice or Nozzle Gas Distributor. *Chem. Eng. Commun.* **1987**, *59*, 201–212.

(41) Tsuge, H.; Nakajima, Y.; Terasaka, K. Behavior of Bubbles Formed from a Submerged Orifice Under High System Pressure. *Chem. Eng. Sci.* **1992**, *47* (13/14), 3273–3280.

(42) Yoo, D. H.; Terasaka, K.; Tsuge, H. Behavior of Bubble Formation at Elevated Pressure. *J. Chem. Eng. Jpn.* **1998**, *31* (1), 76–82.

(43) Yang, G. Q.; Du, B.; Fan, L. S. Bubble formation and dynamics in gas-liquid-solid fluidization—A review. *Chem. Eng. Sci.* **2007**, *62*, 2–27.

(44) Tadaki, T.; Maeda, S. *Kagaku Kogaku* **1963**, *27*, 147.

(45) Azbel, D., *Two-Phase Flows in Chemical Engineering*; Cambridge University Press: New York, 1981.

(46) Leibson, I.; Holcomb, E. G.; Cacoso, A. G.; Jacmic, J. J. Rate of Flow and Mechanics of Bubble Formation from Single Submerged Orifices. *AIChE J.* **1956**, *2* (3), 296–306.

(47) Tsuge, H. Hydrodynamics of Bubble Formation From Submerged Orifices. In *Encyclopedia of Fluid Mechanics*, 1985; Vol. 3, Chapter 9, pp 192−232.

(48) Fan, L. S.; Yang, G. Q.; Lee, D. J.; Tsuchiya, K.; Luo, X. Some Aspects of High Pressure Phenomena of Bubbles in Liquids and Liquid−Solid Suspensions. *Chem. Eng. Sci.* **1999**, *54* (21), 4681–4709.

Received for review April 2, 2008
Revised manuscript received November 13, 2008
Accepted November 13, 2008

IE800516S